

2023

Assessing neurological recovery in post-cardiac arrest comatose patients with diffusion-weighted magnetic resonance imaging

<https://hdl.handle.net/2144/48396>

"Downloaded from OpenBU. Boston University's institutional repository."

BOSTON UNIVERSITY

ARAM V. CHOBANIAN & EDWARD AVEDISIAN SCHOOL OF MEDICINE

Thesis

**ASSESSING NEUROLOGICAL RECOVERY IN POST-CARDIAC ARREST
COMATOSE PATIENTS WITH DIFFUSION-WEIGHTED MAGNETIC
RESONANCE IMAGING**

by

SAM VAN ROY

B.A., Boston University, 2021

Submitted in partial fulfillment of the
requirements for the degree of
Master of Science

2023

© 2023 by
SAM VAN ROY
All rights reserved

Approved by

First Reader

C. James McKnight, Ph.D.
Associate Professor of Pharmacology, Physiology and Biophysics

Second Reader

Jong Woo Lee, MD Ph.D.
Associate Professor of Medicine at Harvard Medical School

**ASSESSING NEUROLOGICAL RECOVERY IN POST-CARDIAC ARREST
COMATOSE PATIENTS WITH DIFFUSION-WEIGHTED MAGNETIC
RESONANCE IMAGING**

SAM VAN ROY

ABSTRACT

Background: Despite advances in healthcare technology and resources, patient survival after cardiac arrest is still very low. Patients who do initially survive cardiac arrest are still at high risk from potentially fatal neurological or other organ injuries (Laver et al., 2004). After initial treatment, clinical care of unresponsive cardiac arrest patients relies heavily on neuroprognostication to assess the extent of brain injury and help form outcome predictions. If neuroprognosis evaluates a patient outcome to be very poor, withdrawal of life-sustaining therapy is likely to occur. These factors make the improvement of neuroprognostication an important challenge in the healthcare industry.

Methods: Our retrospective study constructed and analyzed qualitative and quantitative models of patient neurological outcomes based on diffusion-weighted images (DWI). The patient cohorts included 204 patient post-cardiac arrest comatose targeted temperature management (TTM) patients, as well as a 48-patient non-cardiac arrest control group. Magnetic resonance imaging (MRI) reports were qualitatively assessed for the presence of anoxic injury, while MRI images were quantitatively assessed via their apparent diffusion coefficients (ADC). Models were then constructed based on this data using logistic regression.

Results: Our results indicated that ADC values differed most in cortical regions and that cortical regions quantitatively predicted good patient neurological outcomes superior to all other regions, with only the occipital lobe model having significantly higher predictive value than the qualitative models. We also saw that qualitative models predicted good neurological outcomes with a higher specificity but lower sensitivity than quantitative models. The qualitative and quantitative models showed substantial agreement in most regions, with the qualitative model having a higher positive and lower negative predictive value for good outcomes compared to the quantitative models.

Discussion: We saw a large concentration of anoxic injury in cortical regions, with these regions predicting good patient outcomes better than all others. Generally, the qualitative and quantitative models had the same predictive value across all regions except the occipital lobe. The difference between qualitative and quantitative models seems to provide evidence of a self-fulfilling prophecy in post-cardiac arrest care. Further directions for this project include modeling with the addition of other prognostic tests to form a more valuable predictive model.

TABLE OF CONTENTS

ABSTRACT	iv
TABLE OF CONTENTS	vi
LIST OF TABLES	vii
LIST OF FIGURES	viii
LIST OF ABBREVIATION	ix
INTRODUCTION	1
METHODS	14
RESULTS	24
DISCUSSION	36
CONCLUSION	43
BIBLIOGRAPHY	44
CURRICULUM VITAE	56

LIST OF TABLES

Table 1: Cohort characteristics and demographics	16
Table 2: List of positive outcome classifiers for generation of receiver operating curves	22
Table 3: Area under receiver operating curves values.....	26
Table 4: Validity data of qualatative and quantatative models.....	29
Table 5: Cohen’s kappa values for qualitative and quantitative models	35

LIST OF FIGURES

Figure 1: Flowchart of postresuscitation pathophysiology.....	2
Figure 2: Timeline and phases of post-cardiac arrest syndrome.....	4
Figure 3: Control vs. cardiac cohort anoxic brain injury	24
Figure 4: ROC curve of MRI report models.....	27
Figure 5: ROC curve of whole brain and cortex region models	31
Figure 6: ROC curves all occipital lobe models and group 1 MRI report model.....	33
Figure 7: Distribution of anoxic brain injury.....	37

LIST OF ABBREVIATION

ABI	Anoxic Brain Injury
ADC	Apparent Diffusion Coefficient
AUROC	Area Under the Receiver Operating Curve
CPC	Cerebral Performance Category
DOC	Disorders of Consciousness
DWI	Diffusion-Weighted Imaging
EEG	Electroencephalogram
FSL	FMRIB Software Library
HIBI	Hypoxic Ischemic Brain Injury
MRI	Mass Resonance Imaging
NSE	Neuron Specific Enolase
PCABI	Post-Cardiac Arrest Brain Injury
ROC	Receiver Operating Curve
ROSC	Return of Spontaneous Circulation
SSEP	Somatosensory-Evoked Potentials
TTM	Temperature Targeted Management

INTRODUCTION

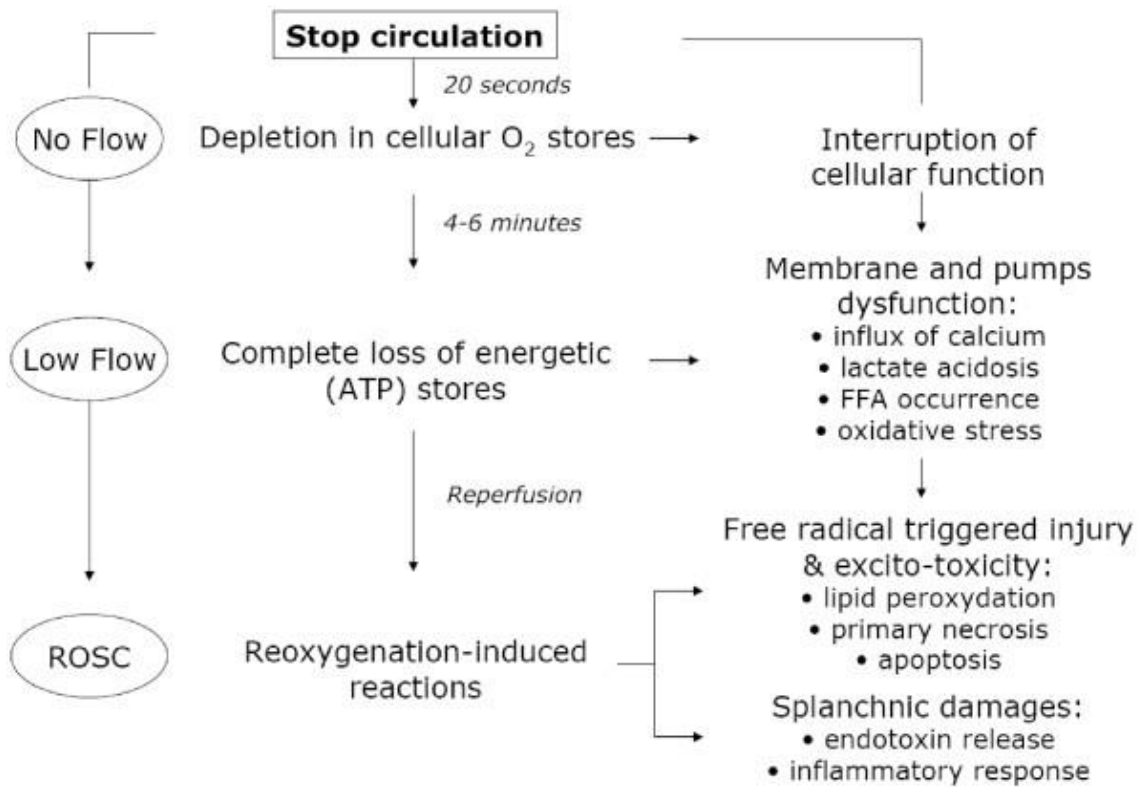
Cardiac Arrest

Cardiac arrest is defined as the mechanical failure of the heart including the absence of systemic circulation for any period. Without the return of systemic circulation, patient death caused by cardiac arrest is inevitable (Gill et al., 2021). These deaths, known as sudden cardiac death, happen within one hour of symptom onset or within twenty-four hours of the patient last seen in usual health. Sudden cardiac death accounts for nearly 9-12% of global mortality, while cardiac arrest accounts for 30% of all global mortality (Mehra 2007). To avoid sudden cardiac death, cardiac arrest is initially treated with cardiopulmonary resuscitation, defibrillation, or both with the intent of returning systemic circulation (Andersen et al., 2019).

Patients who regain circulation after resuscitation are likely to incur potentially fatal neurological injuries caused during the period of no blood flow, known as the anoxic period, or from a reperfusion injury (Laver et al., 2004). The anoxic period is mainly responsible for the primary tissue and cell damage seen in cardiac arrest patients. Initially, the lower metabolic need of the cell balances out the lack of oxygen. But as metabolic needs increase and oxygen levels stay low, plasma membranes depolarize due to low ATP, and mitochondrial membrane potential falls. Eventually, the cell cytoplasm retains enough calcium to cause damage (Mongardon et al., 2011) (Figure 1). When blood flow returns, the formation of radical oxygen compounds begins. One of the most toxic compounds, radical hydroxyl, will increase in concentration enough to cause functional and structural cell lesions and eventually subsequent cell death (Grace 1994)

(Figure 1). This process results in injury referred to as anoxic injury, also known as hypoxic-ischemic injury.

Figure 1. Flowchart of postresuscitation pathophysiology. ROSC - return of spontaneous circulation. (Taken from Monngardon et al., 2011)

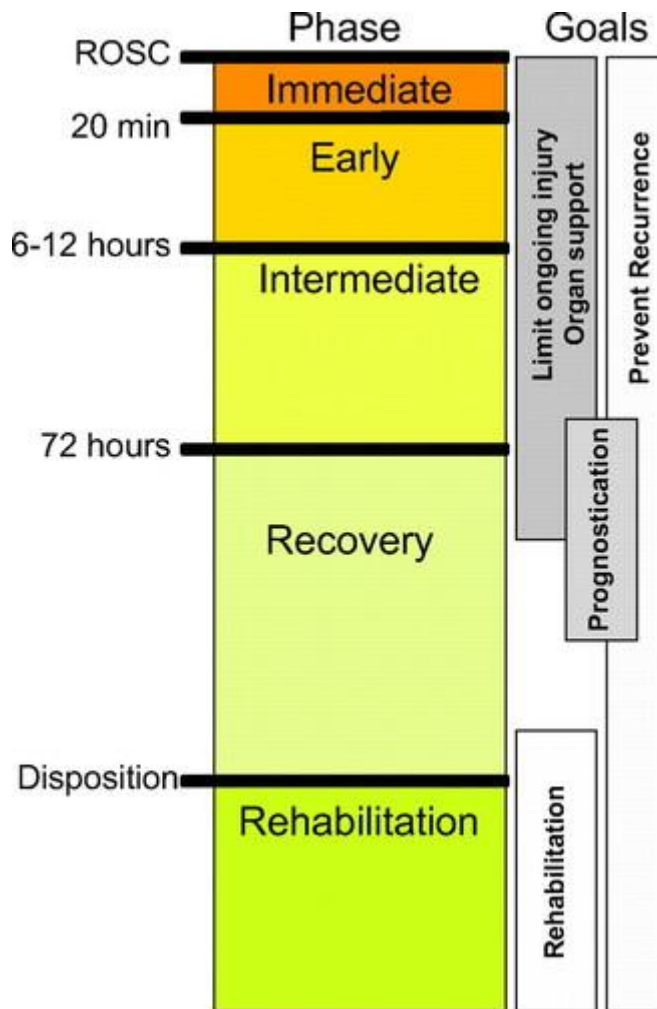


Post Cardiac Arrest Syndrome

Post-cardiac arrest syndrome is a common clinical state that a patient experiences after the survival of cardiac arrest. Symptoms can include a state of shock, myocardial dysfunction, and a high fever due to a sepsis-like inflammatory response. This septic like inflammatory response can result in outcomes such as multiorgan failure and irreparable tissue damage as highlighted in Figure 1 (Nobile et al., 2016). Clinical severity of post-cardiac arrest syndrome outcomes depends greatly on factors including patient health before cardiac arrest, duration of the stoppage of blood flow, other patient comorbidities, and the efficacy of prognostication and treatment (Dalesio 2020).

Treatment during the post-cardiac arrest syndrome period is critical to patient survival and recovery due to the vulnerability of patient health post-cardiac arrest. The initial phase of post-cardiac arrest syndrome is commonly defined as the first 20 minutes post-resuscitation (Figure 2). If a patient is unable to sustain a return of spontaneous circulation for this initial period, care will not be administered (Neumar et al., 2008). Clinical intervention during the early and intermediate phases (Figure 2) is the most crucial due to their efficacy being at its peak. After the first 3 days (Figure 2), prognostic information becomes more reliable which allows clinical outcomes to become more predictable, and treatment becomes focused on long-term patient recovery (Kang 2019).

Figure 2. Timeline and phases of post-cardiac arrest syndrome. (Taken from Nolan et al., 2008)



Neurological Impact of Cardiac Arrest

In a normal resting state, the brain receives a disproportionate amount of blood flow given its small mass compared to the rest of the body. The brain requires around 20% of total cardiac output to maintain homeostasis and any disruption to this blood flow can result in immediate loss of brain activity and subsequent damage (Nolan et al., 2008). It has been observed that during cardiac arrest, a reduction in cerebral oxygen delivery is proportionally greater than the reduction of oxygen transport to the rest of the body. Considering the disproportionate amount of blood flow required by the brain, this can leave it especially vulnerable to ischemic injury during cardiac arrest (Oku 1994).

Within the first 20 seconds of blood flow stoppage to the brain, a person will lose consciousness (Madl and Holzer 2004), within 4 minutes the process of neuronal cell death and neurological injury as shown in Figure 1 will begin, and after 4 minutes without return of spontaneous circulation (ROSC), patient death will occur (Imberti et al., 2003). These injury-causing pathways can happen hours to days post return of spontaneous circulation depending on how long the period of anoxia was. Groups of especially vulnerable neuron populations to apoptosis and necrosis include the hippocampus, cortex, cerebellum, corpus striatum, and thalamus, which leaves the greater structure more vulnerable to injury (Pulsinelli 1985). This neurological injury, known as post-cardiac arrest brain injury (PCABI), hypoxic-ischemic brain injury (HIBI), or anoxic brain injury (ABI), is the leading cause of death in post-resuscitation cardiac arrest patients. The severity and presence of anoxic brain injury is also the primary determinant of long-term disabilities and clinical outcome in patients who survive cardiac arrest

(Sandroni et al., 2021). Less than half of the 10 percent of all cardiac arrest patients surviving until hospital discharge having a full neurological recovery (Grasner et al., 2016). Anoxic injury as we use it in this paper is split into three different categories, cortical, deep gray nuclei structure, and diffuse. Cortical and deep gray nuclei structures are just anoxic injuries present in these structures. Diffuse anoxic injury as it is used here is the presence of anoxic injury in both the cortex and deep gray nuclei structures. Diffuse gray matter anoxic injury is usually associated with severe hypoxic events (Huang and Castillo 2008).

Temperature Targeted Management (TTM)

In an attempt to mitigate the neurological damage caused by the inflammatory response after cardiac arrest, temperature-targeted management (TTM), also known as therapeutic hypothermia, is initiated as soon as possible after the return of spontaneous circulation. With its clinical introduction in 2002, temperature-targeted management has been used in post-cardiac arrest patient care to lower core temperature. Current American Heart Association guidelines recommend all return of spontaneous circulation cardiac arrest patients with abnormal consciousness be cooled for 24 hours once a target temperature of 32 – 36 degrees Celsius is reached (Panchal et al., 2020). Temperature-targeted management lessens the neurological consequences of fever during post-cardiac arrest by slowing cerebral metabolism. This is done in part by decreasing the presence of inflammatory metabolites in the brain (Granfeldt et al., 2021). Other ways in which TTM protects against neuronal injury is by lessening the release of excitatory neurotransmitters

and limiting intracellular apoptotic processes (Yenari and Han, 2012). Many studies have looked at 33 vs 36 degrees Celsius as avoidance of fever target temperatures, however, no differences in neurological outcome have been seen or verified by varying temperatures within this range (Rasmussen et al., 2020). After the 24-hour period of treatment has elapsed, slow rewarming to resting body temperature begins, and treatment to avoid fever continues with pharmacological or nonpharmacological processes (Taccone et al., 2020).

Neuroprognosis

This wide range of clinical outcomes makes prognostic testing and imaging imperative for follow-up care and patient management. Following TTM treatment, various prognostic tests and indicators are used to aid prognosis and improve outcomes. These include tests and indicators such as somatosensory-evoked potentials (SSEP), electroencephalogram (EEG), blood biomarkers such as neuron-specific enolase (NSE), and magnetic resonance imaging (MRI). At the moment, mainly noninvasive imaging is used for prognosis as invasive monitoring has not been proven to be beneficial to patient outcomes (Nguyen et al., 2018).

One early prognostic test is the measurement of SSEPs. SSEPs are measured after eliciting median nerve stimulation. Before TTM, SSEP tests were widely considered to be the most predictive test of neurological outcome (Madl et al., 1996). Cortical SSEPs are still considered to be highly indicative of poor neurological outcomes (Rossetti et al., 2013). However, due to the high false positive rates seen in some studies, other methods have a higher value for neuroprognosis (Howell et al., 2013).

Another useful prognostic test, EEG, has been shown to be highly discriminative of good neurological patient outcomes at normothermia (Westhall et al., 2016). EEG works by measuring electrical activity in the human brain thought to be from cortical surface neurons primarily (Britton et al., 2016). However, due to studies confirming EEG's limited ability in predicting poor patient outcomes, guidelines recommend that malignant patterns be considered in conjunction with another prognostic testing (Sandroni et al., 2018).

Blood biomarkers also play a significant role in neuroprognostication. After cardiac arrest, breakdown products from neurons and astrocytes can be measured in serum as indicators of anoxic injury (Cronberg et al., 2020). Products such as neuron-specific enolase (NSE) have been shown to significantly increase after an anoxic brain injury. NSE at high concentrations has been shown to have a reasonable performance in prognostic testing (Stammet et al., 2015), but is limited by many factors such as contamination by hemolysis (Stern et al., 2007).

While computed tomography scans and conventional MRI are useful in assessing the extent of injury regarding brain structure, they are not utilized to assess acute injury during neuroprognosis because they often underplay the extent and severity of injury (Choi et al., 2010). Diffusion-weighted imaging (DWI) however, can be especially useful in these situations to assess the extent of acute injury. DWI, which is dependent on the motion of water molecules within the brain, also gives quantitative measures of brain damage known as the apparent diffusion coefficient (ADC). A reduction in ADC or percent of tissue with a reduced ADC value has been seen to hold predictive value in

patient neurological outcomes (Sener et al., 2020). Agreed-upon thresholds for ADC values to predict outcomes have not been thoroughly validated by the medical community. However, in practice radiologists will typically refer to an ADC value below 700-850 x 10⁻⁶ mm²/s for deep gray matter and 800-1000 x 10⁻⁶ mm²/s for cortical gray matter as an indication of injury (Helenius et al., 2002). In conjunction with other clinical factors and knowledge, ADC values help guide radiologists in their final interpretation of a brain MRI.

Neurological Outcomes Post Anoxic Brain Injury

Patients can incur a wide array of outcomes after the initial survival from an anoxic brain injury. This includes outcomes such as a full neurological recovery, mild to severe disabilities, or a persistent vegetative state (Hoiland et al., 2022). The most frequently damaged regions of the brain include the hippocampus, cerebral cortex, thalamus, and cerebellum which can cause disorders of consciousness, seizure, and stroke (Geocadin et al., 2008). The presence of these disorders of consciousness (DOC) can be strongly indicative of a poor neurological outcome (Kamps et al., 2013).

Disorders of consciousness include coma, vegetative state, and minimally conscious state (Forgacs et al. 2020). Nearly 80 percent of cardiac arrest survivors remain in a comatose state in the period initially post-cardiac arrest (Sandroni et al., 2021), with 79% of these patients experiencing detrimental long-term neurological outcomes (Kamps et al., 2013). Damage to the thalamocortical network or bilateral cortical regions is also responsible for common poor long-term neurological outcome presentations ranging from

memory deficit to persistent vegetative state (Nolan et al., 2008). Many survivors of cardiac arrest have been observed to develop psychological issues such as anxiety, depression, and PTSD, as well as physical disabilities such as vision, hearing, speech, mobility, and dexterity impairment and overall pain (Schaaf et al., 2012). Autonomic center injuries, like hypothalamic or hypothalamic tract injury, can cause paroxysmal autonomic instability with dystonia, a condition including a wide range of clinical symptoms ranging from hypertension to agitation (Blackman et al., 2004).

Self-fulfilling Prophecy and Other Possible Bias

Medical errors serve as a large cause of morbidity and mortality in the United States, with high estimates attributing these errors as the third largest cause of death (Markay and Daniel 2016). Generally, these errors can be placed into the following different categories; diagnostic, treatment, preventative, equipment, or system errors (Kohn 2000). In radiology, errors are usually diagnostic. These diagnostic errors can result in incorrect, delayed, or omitted diagnoses (Lee et al., 2013). Biases and other psychological phenomena such as self-fulfilling prophecy can play an important role in the production of these diagnostic radiology errors.

One important psychological factor that may impact the clinical outcome for patients recovering from cardiac arrest is the role of a self-fulfilling prophecy. Self-fulfilling prophecy refers to the concept of how our previous notions about others can affect our treatment of them in a way that will subsequently make the other person become what we think them to be (Macrae and Quadflieg 2020). If providers and other

members of a patient's care team perceive that patient outcomes will be poor, treatment and prognosis may be adversely affected to reflect this belief. One example of the impact that a self-fulfilling prophecy may have on cardiac arrest patients is limitations on further resuscitation as well as withdrawal of life-sustaining therapy timing. In one study where 53% of patients were withdrawn from therapy only 48 hours post-return of spontaneous circulation, well before an accurate prognosis of neurological recovery could be soundly established (Grossestreuer et al., 2016). Another study found that the majority of deaths post-return of spontaneous circulation were due to the withdrawal of life-sustaining therapy in response to a poor neurological outcome prognostication (Dragancea et al., 2017). Self-fulfilling prophecy can also strengthen the test that is used to determine the outcome in the first place, further compounding its impact. Taking the previous example of withdrawal of care, retrospective studies show certain factors used to previously determine withdrawal of care will strongly correlate with the outcome.

Another possible influence of bias on post-cardiac arrest patient care is during prognostication, more specifically the role of anchoring bias when radiologists read MRI images and generate reports. Anchoring bias explains the situation where, in this case, a radiologist may fixate on his/her initial impression of diagnosis, regardless of the presence of contradicting information (Waite et al., 2017). Due to anchoring bias, radiologists may feel more inclined to report that brain injury is more severe in patients if these radiologists initially predicted poorer clinical outcomes/the presence of anoxic injury in the patient. This can have major impacts on a patient's plan of care, as a patient care team relies heavily on prognosis reports to develop a care plan.

Our Study

In this thesis, we aim to assess neurological recovery in post-cardiac arrest comatose TTM patients. We will use diffusion-weighted images to build and train quantitative prediction models for specific brain regions. We will qualify the reports of the diffusion-weighted images used for analysis and use this data to build and train a qualitative prediction model. We will then analyze and compare the quantitative and qualitative models' separate predictive values. We hypothesize that gray matter structures, specifically cortical and deep gray nuclei structures, will build better quantitative models due to the prior mentioned vulnerability to anoxic injury. We predict that the qualitative reports will generally be more accurate than the quantitative models but might have lower specificity for good outcomes due to the influence of self-fulfilling prophecy.

Specific Aims

The specific aims of this thesis include the following:

1. Assess the accuracy of radiological readings and apparent diffusion coefficient values of diffusion-weighted imaging sequences in predicting neurological outcomes.
2. Compare the strengths and weaknesses of radiological readings and apparent diffusion coefficient value models in predicting neurological outcomes.
3. Investigate the presence, if any, of bias in radiological reporting regarding neuroprognostication of post-cardiac arrest anoxic injury patients.

4. Assess whether including a quantitative prediction model can help improve neuroprognostication in post-cardiac arrest anoxic injury patients.

METHODS

Raw data was collected and provided by Snider et al., 2022 with permission from Samuel B. Snider, MD of Brigham and Women's Hospital. MRI registration and control vs. cardiac cohort analysis were done by Snider et al., 2022. The processed MR images were used to create models and statistically verify data.

Standard Protocols, Approvals, Registration, and Patient Consent

Data collection from Snider et al. was approved by the Mass General Brigham institutional review board under protocols 2014P001623 and 2021P000633. The requirement for participant consent was waived for the study.

Cardiac Arrest Cohort

The selection of the cardiac arrest cohort and data retrieval was performed by Snider et al., 2022. In the initial selection, 573 patients were picked from a Brigham and Women's Hospital registry of in-hospital and out-of-hospital cardiac arrest patients between 2009 and 2020. Patients included in this study were over 18 years of age and had not followed commands upon assessment by the attending neurologist after the return of spontaneous circulation (ROSC). At Brigham and Women's Hospital, patients who are unresponsive within 72 hours of admission due to cardiac arrest and have the required stability for an MRI are commonly ordered one. Of these 573 patients selected, only 206 patients had a diffusion-weighted MRI within 14 days of cardiac arrest.

Basic demographic information, the use of targeted temperature management (TTM), and the time between cardiac arrest and acquisition of diffusion-weighted imaging MRI were extracted from the hospital's electronic medical record system (Table 1). Targeted temperature management was administered on unresponsive patients post-resuscitation as per the hospital's protocol. The core temperature targeted used was 33 degrees Celsius and was recorded via a bladder probe. Lowering core temperature was achieved via cooling pads used for a 24-hour period. If clinical limitations arose that did not allow a 33-degree Celsius target to be reached, such as a hemorrhage, a target of 36 degrees Celsius was used. Patients with any missing data were excluded from the analysis.

Table 1. Cohort characteristics and demographics. CI, confidence interval; TTM, targeted temperature management. (Taken from Snider et al., 2022)

	Patients with cardiac arrest (n = 204)	Controls (n = 48)	<i>p</i> Value
Mean age (95% CI), y	55 (53, 58)	51 (47, 55)	0.04
Male sex, n (%)	131 (64)	13 (27)	<0.001
White ethnicity, n (%)	130 (64)	36 (82)	0.04
Received TTM, n (%)	176 (86)		
Followed commands before discharge, n (%)	80 (39)		
Died before discharge, n (%)	116 (58)		
Mean days between arrest and MRI (95% CI)	5.0 (4.6, 5.3)		

MRI Processing and Information

MRI processing was done by Snider et al., 2022. The initial post-cardiac arrest diffusion and T1 sequences were used for analysis. Other images regarding a different date or sequence type were not included in this study. All acquired diffusion sequences followed specific parameters such as $b = 0, 500, 1,000$ seconds/mm², 1.5 x 1.5 x 6 mm voxel size, and diffusion encoding along the principal axes. Acquired T1-weighted sequences included sagittal and axial pre-contrast volumes (voxel size around 0.5 x 0.5 x 5 mm) or a magnetization-prepared rapid gradient echo volume (voxel size 1 x 1 x 1 mm).

Quantitative analysis of the ADC maps was done via diffusion-weighted sequences. During the registration of the MRIs, ADC maps were registered into a standardized space. Brain extraction was performed using FMRIB Software Library (FSL) and bet2 and merged linear, nonlinear, and diffeomorphic registrations using ANTs:antsRegistrationSyNQuick. This was done between the diffusion b0 volume, the T1-weighted MRI, and the Montreal Neurological Institute 152 T1 space. The above process was accomplished using code acquired from GitHub (Ebner et al., 2020). When a T1-weighted isotropic magnetization-prepared rapid gradient echo sequence was unattainable or not produced, the clinical sagittal and axial T1 volumes were used. To prepare them for use, the sagittal and axial volumes were bias-field corrected and resliced to produce an isotropic T1 volume. The isotropic T1 volume was later enhanced to a higher resolution volume using NiftyMIC (Ebner et al., 2020). NiftyMIC accomplishes this using a two-step iterative model including rigid slices to volume registration and

cycles of robust resolution reconstruction (Ebner et al., 2020). Every registration was also inspected manually via slicesdir (FSL 6.0.1). After inspection, only two MRIs were excluded. These exclusions were due to the registrations of gross inaccuracy.

The ADC maps produced excluded any values outside of the range of 200 to $1,200 \times 10^{-6} \text{ mm}^2/\text{s}$ to mitigate artifact and cerebrospinal fluid signal contribution. The threshold used was based on previous works done in the field (Beveris et al., 2018) (Hirsh et al., 2020). The above transformations were then applied to the ADC maps to translate them into the Montreal Neurological Institute space for comparison.

Non-Cardiac Arrest Control Group

Data collection of the control group was performed by Snider et al., 2022. A patient cohort that did not have significant brain pathology was created as a control group. The purpose of this group was to test whether ADC values in the cardiac arrest cohort differed significantly from non-pathological brain readings. Formation of the control group was done by filtering for patients with MRI reports in the electronic medical record system that contained “migraine headaches”. All MRI ‘s had been performed between 2000 and 2020 in this patient cohort. Out of the more than 6000 patients returned by the search, 150 were randomly selected. Of the 150 patients, 57 patients were within our institution and hence compatible with the patients from the cardiac arrest cohort. The brain MRIs of these 57 patients were processed with the same procedure as above. 9 patients were excluded due to missing data, diffusion sequence, T1

sequence, or grossly inaccurate registrations. This left 48 patients in the control group (Table 1).

Region of Interest ADC Measurements

Mean ADC values were calculated for each patient within the region of interest. This was done by transforming binary Montreal Neurological Institute space regions of interest onto patients' ADC maps and taking the average ADC value of the region. Regions of interest for gray matter were the bilateral frontal, temporal, insular, parietal, and occipital lobes, as well as the cerebellum based on the MNI Structural Atlas (Collins et al., 1994). Gray matter regions of interest also included the bilateral basal ganglia (including the caudate, putamen, and pallidum), bilateral thalamic, and brainstem based on the Harvard-Oxford Subcortical Atlas (Makris et al., 2007) (Frazier et al., 2005) (Desikan et al., 2006) (Goldstein et al., 2007). White matter regions of interest included the bilateral and binarized tracts and the corpus callosum based on the Johns Hopkins University White Matter Atlas (Mori et al., 2005) (Wakana et al., 2007) (Hua et al., 2008) and Jülich Atlas (Eickhoff et al., 2005, 2006, 2007) respectively.

MRI Report Qualification

MRI reports associated with the MRI images of the cardiac cohort used for analysis were retrieved from the Brigham and Women's electronic medical record database. The reports were qualified with grades of 1 to 4 to provide data for further analysis. A grade of 1 was assigned to indicate diffuse anoxic injury, 2 for cortical anoxic

injury only, 3 for thalamus and/or basal ganglia anoxic injury only, and 4 for no anoxic injury. MRI reports with any indication of cortical, basal ganglia, or thalamus anoxic brain injury received the respective grade. MRI reports with an indication of diffuse anoxic injury or that included mentions of both cortical and deep gray nuclei structure anoxic injury were classified as diffuse anoxic injury. The MRI report qualification was done as shown above due to previous studies showing the high vulnerability and predictive values of cortical and deep gray nuclei structures (Lacerte et al., 2022) (Choi et al., 2016).

Qualitative and Quantitative Model Construction and Analysis

To compare how well mean ADC values of their respective regions of interest and MRI reports could classify patient neurological outcomes, we generated and analyzed receiver operating characteristic (ROC) curves. Receiver operating curves and logistical regression models were produced using the R package pROC (Robin et al., 2011) and ROCR (Sing et al., 2005). To train the logistic regression model, we binarized patient outcomes into good or poor neurological outcomes by either using the cerebral performance category (CPC) or whether a patient followed commands upon assessment.

The logistic regression model used the provided ADC or MRI report data to predict the patient outcome by using continuous ADC thresholds from $200 - 1200 \times 10^{-6} \text{ mm}^2/\text{s}$ or MRI grades for each respective model to predict patient outcome as good/poor. By comparing the outcome prediction with the actual good/poor neurological outcome specific to the testing group, it calculated sensitivity and specificity for each

threshold and produced a receiver operating characteristics curve based on these points. Models were built to predict good neurological outcomes in patients, so sensitivity and specificity reflect predictions of good neurological outcomes.

For positive classifiers of good outcomes throughout the analysis, the values listed in Table 2 were used. Cerebral performance category scores and following commands are neurological assessments taken 6 months post-hospital discharge. These scores are given as assessments of long-term and functional neurological outcomes (Reynolds and Soar, 2005). A cerebral performance category score of 1-2 (group 1) is clinically considered a good neurological outcome, patients in this category can function independently for most tasks. A CPC score of 1 indicates a patient with no more than minor neurological deficits. A CPC score of 2 indicates patients with mild neurological disabilities, someone who is still independent but may suffer from seizures, memory loss, etc. (Ajam et al., 2011). A CPC 1-3 (group 2) was used to qualify a good outcome as anybody able to recover beyond a comatose or vegetative state, as a CPC score of 3 is given to those with severe neurological disabilities and a score of 4 is given to those in a coma/persistent vegetative state. Following commands (group 3) was used to attempt to exclude patients who fall under a CPC score of 5, classified as brain dead, who may recover neurologically but later died in the hospital due to other clinical factors (Reynolds and Soar, 2005).

Table 2. List of positive outcome classifiers for generation of receiver operating curves.

	Positive Outcome Classifier
Test Group 1	Cerebral Performance Score 1-2
Test Group 2	Cerebral Performance Score 1-3
Test Group 3	Follows Commands Upon Evaluation

We compared the areas under the ROC curve (AUROC) of the ADC mean value models and MRI report models using the Delong test. Maximum sensitivity and specificity for each test were retrieved from the ROC curve and positive and negative predictive values were calculated.

These thresholds were then used to binarize patient outcome predictions to calculate the Cohen's Kappa value for each test. The Cohen's kappa value was used to measure the degree of agreeability between the two predictive tests in each respective region of interest. The calculated thresholds were then used to binarize the outcome data, any MRI with an ADC value above the calculated optimal threshold would be classified as a good outcome prediction (value of 1) by the quantitative model, and any MRI report with a grade of 1-3 would be classified as a good outcome prediction (value of 1) by the qualitative model. The number of agreements/disagreements was then able to be counted and Cohen's kappa was calculated.

In another part of our analysis, qualitative and quantitative model sensitivities for good outcomes were individually forced to 100% and the correlating specificity and optimal threshold were retrieved. Specificity, optimal threshold, and Cohen's kappa

values were calculated when sensitivity for good outcome was at 100% for qualitative and quantitative models. This was done to create a predictive model that would not falsely predict poor neurological outcomes.

RESULTS

Description of Study Cohort

Patient population characteristics are shown in Table 1. The cardiac arrest cohort was slightly older than the control group with a mean age of 55. This cohort had a larger proportion of men and participants identifying not as white than the control population. ADC value distribution of the cardiac cohort and the control group were compared to indicate which region of interest is most affected by post-cardiac arrest anoxic brain injury, as well as to verify a significant difference in mean ADC values. Mean cortical ADC values were significantly lower in the cardiac cohort compared to the control (Figure 3). Mean occipital lobe ADC values were significantly the lowest across all regions of interest.

Figure 3. Control vs. Cardiac Cohort Anoxic Brain Injury. Voxels with significantly lower mean ADC values in patients with cardiac arrest compared to controls are highlighted below. (Taken from Snider et al., 2022).



Qualitative MRI Report-Based Models

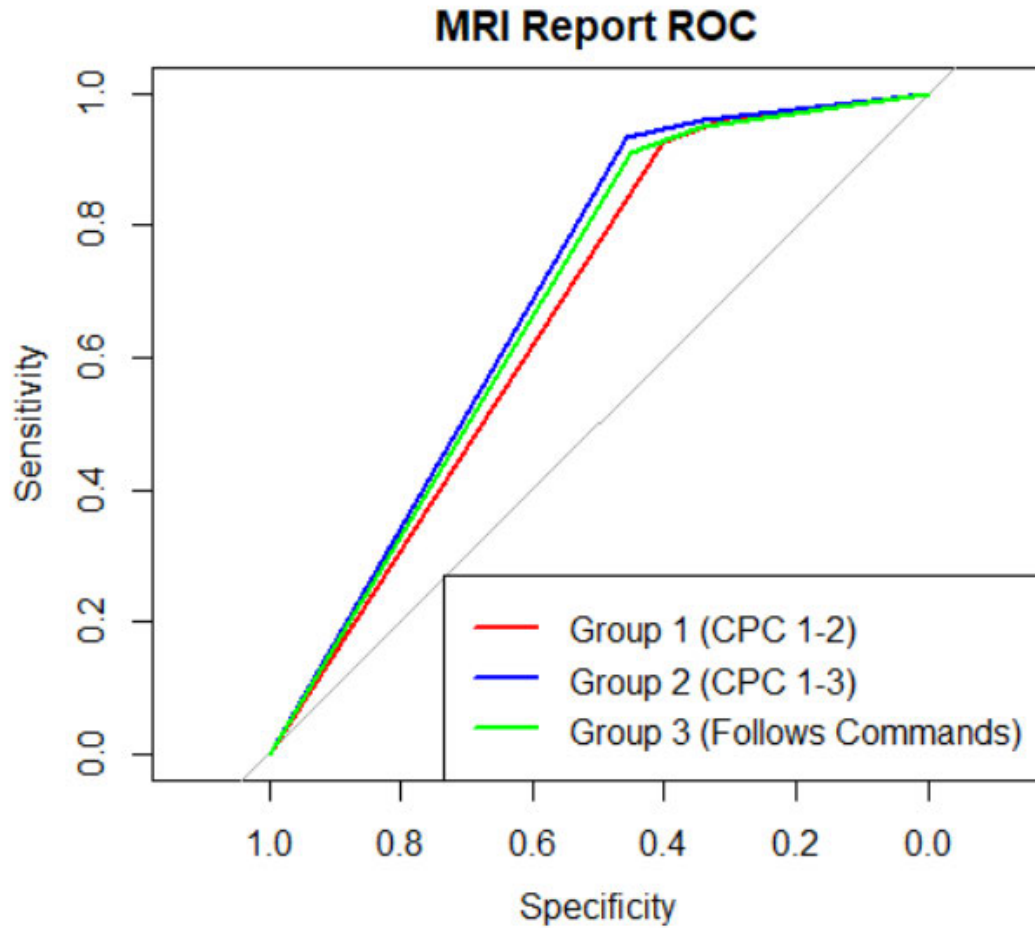
The cardiac cohort included 204 patients for analysis. From qualifying patient MRI reports we saw that 88 patient MRI reports (36.7%) indicated no anoxic injury, 135 (66.2%) indicated diffuse anoxic injury, 17 (7.1%) indicated cortical-only anoxic injury, and none indicated deep gray nuclei-only (basal ganglia and thalamus) anoxic injury. Receiver operating curves were generated for all regions of interest in the cardiac cohort.

To assess how the predictive value of our models changes when neurological outcome classification varies, AUROC was calculated and compared via DeLong's test for each model. The AUROC for the MRI report models are as listed in Table 3. All MRI report models, regardless of region of interest, used the same data due to each MRI report only being assigned one grade. So, as we expected, the MRI report models only varied when changing outcome classifiers/testing groups and not with regions of interest. The MRI report model for test group 3, which used the cerebral performance score of 1 to 3 to classify good neurological outcomes (Table 2), had the highest AUROC of 0.698 (Figure 4).

Table 3. AUROC curves values. Any AUROC that was below the whole brain was omitted from this table.

Model type	Area Under Receiver Operating Curve		
	Test Group 1 (CPC 1-2)	Test Group 2 (CPC 1-3)	Test Group 3 (Follows commands)
MRI Report	0.669	0.698	0.685
Occipital Lobe	0.712	0.767	0.767
Parietal Lobe	0.680	0.731	0.727
Whole Cortex	0.679	0.725	0.726
Forceps Major	0.650	0.723	0.715
Whole Brain	0.649	0.698	0.702
Average of All ROI	0.596	0.635	0.637

Figure 4. ROC curve of MRI report models. No significant difference between the different testing groups AUROC and optimal sensitivity and specificity. The optimal threshold for all groups was calculated to be a grade of 1 (diffuse anoxic injury). Generated using the pROC package in RStudio (Robin et al., 2011).



The group 2 MRI report model also had the highest sensitivity and specificity out of all the MRI report models at 93.3% and 45.7% respectively (Table 4). The group 2 MRI report models also had the highest positive and negative predictive values (Table 4). However, there was only a slight variation between all test groups (Figure 4). Delong's test showed that there was no statistical difference in AUROC between all MRI report test groups ($p > 0.05$). The optimal threshold for MRI report grade to classify patient outcome was a grade of 3 for all three test groups (Figure 4), meaning all scores besides 4 (no anoxic injury) predicted poor neurological outcome according to this model.

Table 4. Validity data of qualitative and quantitative models. The sensitivities, specificities, positive predictive values (PPV), and negative predictive values (NPV) for good outcome from the qualitative and quantitative models. The sensitivity and specificity data were retrieved from the receiver operating curves generated for analysis.

Model Type	Testing Group 1 (CPC 1-2)				Testing Group 2 (CPC 1-3)				Testing Group 3 (Follows Commands)			
	Sensitivity	Specificity	PPV	NPV	Sensitivity	Specificity	PPV	NPV	Sensitivity	Specificity	PPV	NPV
MRI Reports	92.70%	40.30%	95.70%	33.70%	93.30%	45.70%	93.60%	45.80%	91.00%	45.20%	91.50%	47.10%
Occipital Lobe	76.40%	57.00%	86.70%	39.60%	81.30%	65.10%	85.70%	57.50%	80.80%	65.90%	84.70%	59.40%
Parietal Lobe	72.70%	55.00%	84.50%	37.40%	77.30%	62.00%	82.50%	54.20%	79.50%	60.30%	82.60%	55.40%
Whole Cortex	74.50%	57.00%	85.90%	39.00%	80.00%	59.70%	83.70%	53.60%	78.20%	60.30%	81.70%	55.00%
Whole Brain	72.70%	54.40%	84.40%	37.00%	74.70%	59.70%	80.20%	51.90%	74.40%	60.30%	91.50%	47.10%

+



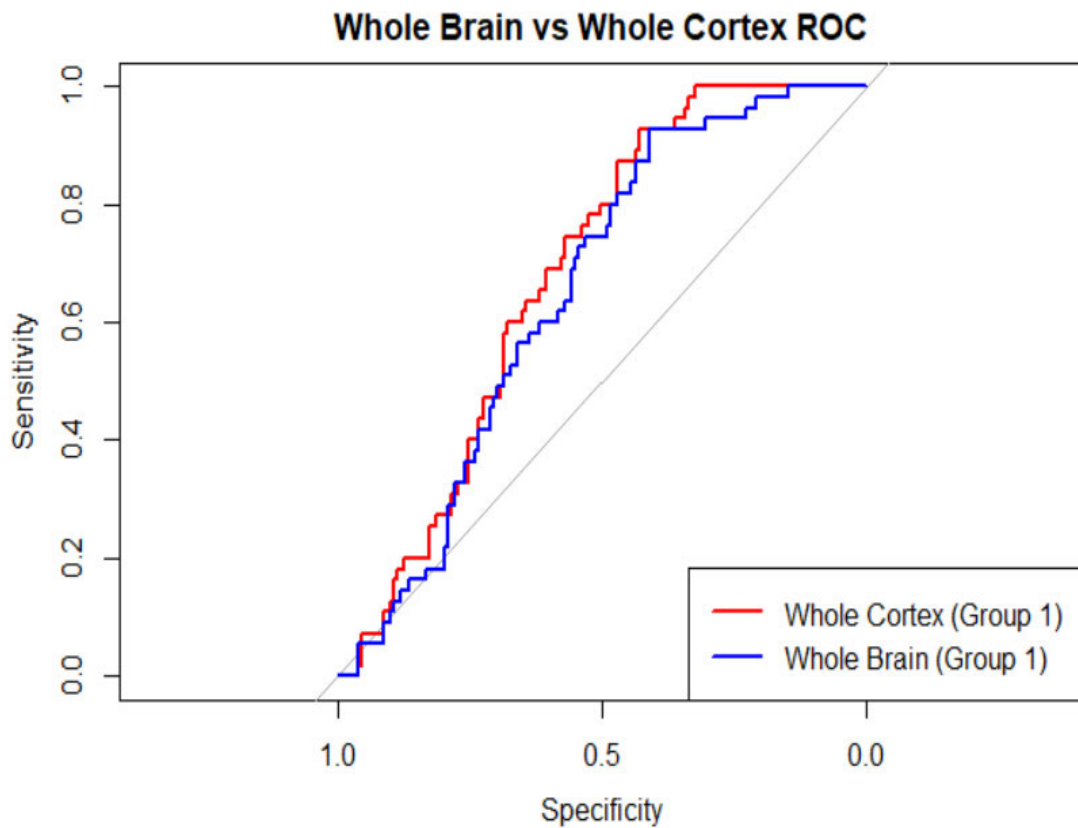
Quantitative ADC Value-Based Models

Receiver operating characteristic curves were generated for all regions of interest in the cardiac cohort. To assess how the predictive value of our ADC value-based models changes when neurological outcome classification and region of interest varies, AUROC was calculated and compared via Delong's test for each model. The average region of interest AUROC for the group 3 ADC value models was the highest amongst all 3 groups at 0.637, with a whole brain model AUROC of 0.702 (Figure 5). Cortical structure models generally showed the highest accuracy in classifying patient outcomes. The whole cortex region model predicted outcome better than the whole brain model, with the whole cortex region model AUROC being significantly larger compared to the whole brain region across all testing groups ($p < 0.05$) (Figure 5).

The occipital lobe, whole cortex, and parietal lobe ADC value models had the three highest AUROC across all testing groups (Table 3). However, the frontal lobe model and temporal lobe model AUROC remained lower than the whole cortex model AUROC across all groups. The forceps major region model AUROC was within the fifth highest across all groups. The occipital lobe region model had the highest AUROC of 0.712, 0.767, and 0.767 for group 1, group 2, and group 3 respectively (Table 3). Using Delong's test, we saw that the occipital lobe region model AUROC was significantly higher than the second highest AUROC (parietal lobe) in groups 1 and 2 but not in group 3 ($p < 0.05$). The occipital lobe mean ADC value test also had the highest sensitivity and specificity, and positive and negative predictive values of all ROI mean ADC values models (Figure 6) (Table 4). The deep gray nuclei structure regions AUROCs, bilateral

basal ganglia and thalamus, were significantly less than whole cortex AUROC across all testing groups ($p < 0.05$).

Figure 5. ROC curve of whole brain and cortex region models. The whole cortex ADC value model was significantly higher across all groups. Whole cortex and whole brain model sensitivity and specificity are listed in Table 4. The whole cortex and whole brain optimal thresholds are $840.3 \times 10^{-6} \text{ mm}^2/\text{s}$ and $820.0 \times 10^{-6} \text{ mm}^2/\text{s}$ respectively. Generated using the pROC package in RStudio (Robin et al., 2011).

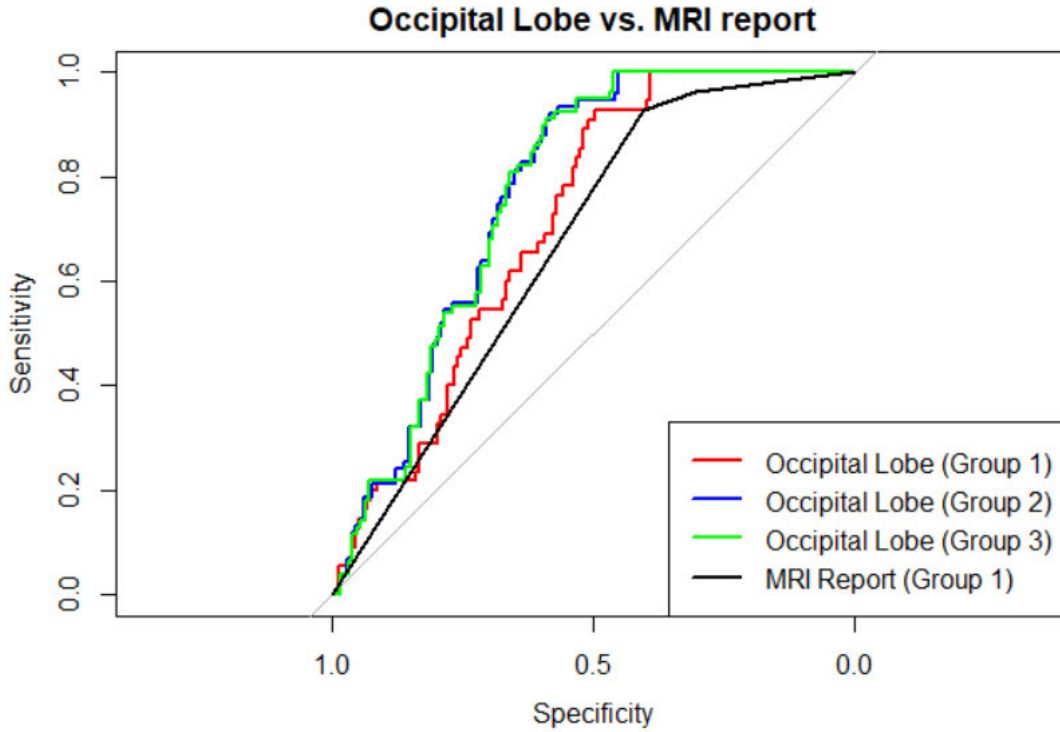


Statistical Comparison of Qualitative and Quantitative Models

The whole brain ADC value model AUROC did not differ significantly from the MRI report models' AUROC in all testing groups ($Z < 1$, $p > 0.05$). The group 2 MRI report model's AUROC was the highest out of all MRI report models (0.696), while the AUROC of the group 3 whole brain model was larger than the group 1 or 2 whole brain model's AUROC (0.702). Out of all the ADC value models, only the occipital lobe, parietal lobe, and cortex-only region models had AUROCs higher than the MRI report models across all testing groups (Table 3). However, out of these models, only the testing group 3 (follows commands) occipital lobe region model's AUROC (0.766) was significantly higher than the same group MRI report model's AUROC (0.685) (DeLong $p = 0.043$, $Z = 2.02$) (Figure 6).

Qualitative model sensitivity for a good outcome was higher and specificity for a good outcome was lower than quantitative models across all testing groups and regions (Table 4). Qualitative models typically had higher positive predictive values (~ 20% higher) and lower negative predictive values (~ 10% lower) across all testing groups when compared to the best-performing quantitative models. The group 2 qualitative model had the highest positive predictive values across all groups, while the group 2 occipital lobe model had the highest negative predictive value across all groups (Table 4).

Figure 6. ROC curves all occipital lobe models and group 1 MRI report model. Only the group 3 occipital lobe model had a statistically higher AUROC than the MRI report model. Only the group 1 MRI report model was included due to the lack of statistical difference between the 3 groups. AUROC are as reported in Table 3.



Average Cohen’s kappa values in all 3 testing groups showed a moderate level of agreement between the ADC value models and MRI report models, with all average Cohen’s kappa values being equal to 0.0575 ± 0.03 (Table 5). The group 3 occipital lobe and MRI report models had a substantial agreement with a Cohen’s kappa value of 0.63 (Table 5). Surprisingly, the occipital lobe region models did not have the highest Cohen’s kappa value in any of the 3 testing groups, despite showing the most predictive value out of any of the ADC value models. The forceps major model had the highest Cohen’s

kappa value in groups 1 and 3 with the forceps minor model having the highest Cohen's kappa value in group 2 (Table 5). The whole cortex model showed substantial agreement in both groups 2 and 3 but only moderate agreement in group 1 (Table 5).

When sensitivity was forced to 100%, we saw that the specificities for our best-performing models, the occipital, parietal, and whole cortex, resulted in an average specificity of 43.3%, 39.6%, and 35.8% respectively. The quantitative model specificity was significantly higher than the qualitative model specificity at 100% sensitivity. The qualitative model specificities were 28.3%, 34.2%, and 33.9% for testing groups 1-3 respectively. The occipital region model performed the best with a specificity of 46% in group 3 when sensitivity was at 100%. The Cohen's kappa value increased slightly when sensitivities were set at 100%. A Cohen's kappa value increase to 0.68 was seen across all regions of interest and testing groups, as an increase to the 100% sensitivity ADC threshold changed all quantitative predictions to be a good neurological outcome.

Table 5. Cohen’s Kappa values for qualitative and quantitative models. Cohen’s kappa value measures agreeability between two independent raters. A Cohen’s kappa value of 0.01–0.20 represents none too little, 0.21–0.40 represents fair, 0.41– 0.60 represents moderate, 0.61–0.80 represents substantial, and 0.81–1.00 represents nearly perfect agreement (McHugh 2012).

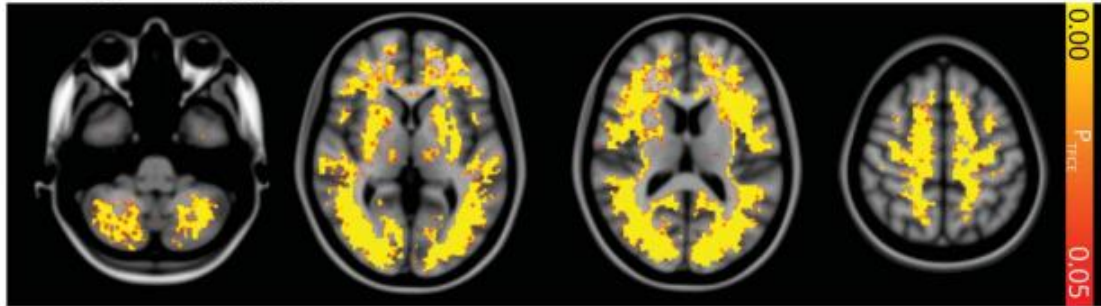
Model Region of Interest	Cohen’s Kappa Value		
	Test Group 1 (CPC 1-2)	Test Group 2 (CPC 1-3)	Test Group 3 (Follows commands)
Forceps Major	0.644	0.599	0.649
Occipital Lobe	0.629	0.629	0.629
Parietal Lobe	0.574	0.574	0.599
Whole Cortex	0.594	0.619	0.614
Forceps Minor	0.644	0.644	0.589
Whole Brain	0.589	0.589	0.589
Average of All ROI	0.577	0.579	0.575

DISCUSSION

Assessment of Quantitative Predictive Model

We found that cortical region ADC value-based models tended to perform significantly better as predictive models of neurological patient outcomes than the whole brain and other regions of interest models. These findings are understandable as the severity of gray matter injury has been shown to be highly correlated with patient outcomes (Figure 7) (Choi et al., 2016). This can partly be attributed to the vulnerability of cortical neurons to anoxic injury and the importance of cognitive function on the outcome (Lacerte et al., 2022). Snider et al.'s study also confirms the strong correlation in our patient cohort between cortical mean ADC value reduction and poor neurological outcome (Snider et al., 2022). This could be explained by regional differences in metabolic demand or perfusion (Ishii et al., 1996). This vulnerability was also highlighted with cortical ADC values being significantly lower in cardiac arrest patients compared to controls (Figure 3). Another region particularly vulnerable to anoxic brain injury is the hippocampus (Endisch et al., 2020). However, hippocampal models did not prove to be particularly effective and hippocampal mean ADC values did not differ substantially from controls. This could be due to the limitations of diffusion-weighted imaging on discriminating structures in the mesial temporal lobe (Verduin et al., 2021).

Figure 7. Distribution of Anoxic Brain Injury. Voxel-wise distribution of ADC values between recovered and non-recovered cardiac arrest patients. Cortical structures showed a significantly lower reduction in ADC values in patients who did not recover from cardiac arrest. (Taken from Snider et al., 2022).



We saw that the occipital lobe region model predicted neurological outcomes significantly better than the whole brain model and all other regional models. The occipital lobe model results can be explained by findings that demonstrate the primary visual cortex to have the highest resting metabolic rate in the brain (though still disputed) (Shokri-Kojori et al., 2019). Therefore, we would expect the occipital lobe to be very susceptible to the metabolic changes of anoxic brain injury highlighted in Figure 1.

The parietal lobe model also showed to have predicted neurological outcomes significantly better than the whole brain model, with the second highest AUROC for two of the three testing groups. However, the frontal and temporal lobe models did not prove to be of high relative value compared to the parietal and occipital lobe models. One possible explanation for the variation of model accuracy in the cortical region is the theory that the posterior predominance of anoxic injury (as seen in the decreased ADC values in Figure 6) is similar to posterior reversible encephalopathy syndrome. Specifically, during the cardiac arrest the body fails to autoregulate and maintain

perfusion at low pressures, like in posterior reversible encephalopathy syndrome when the body fails to autoregulate and limit blood flow at high pressure (Snider et al., 2022).

Other gray matter structure models did not perform as well as cortical structures in predicting outcomes. One study found results consistent with ours, that deep gray nuclei structure models performed less specifically as compared to cortical models (Hirsch et al., 2015). Surprisingly, however, the deep gray nuclei structures (basal ganglia and thalamus) models performed consistently worse than the whole brain model. This is contrary to one study that found the ADC values of these structures correlate with trends in patient outcomes (Mlynash et al., 2010). One possible explanation could be the lack of deep gray nuclei structure-only injury patients in our cardiac cohort, with no MRI reports being qualified as basal ganglia/thalamus anoxic injury only. However, a significant number of patients (66.2%) were reported as having a diffuse anoxic injury, many of which included injury to deep gray nuclei structures. Another possible explanation could be in the timing of our images. Our study sampled only the most recent image to cardiac arrest, which is taken 72 hours post-cardiac arrest per hospital protocols. Whereas Mlynash et al.'s study sampled images 3 to 5 days post cardiac arrest and monitored ADC values throughout this period to establish a trend (Mlynash et al., 2010).

Assessment of Qualitative Prediction Models

As stated before, MRI report models did not differ significantly between testing groups. In these models, sensitivity for good neurological outcomes was high (> 90%) specificity for good neurological outcomes was quite low (< 50%), (Table 4). The low

specificity is reasonable, as in practice during neuroprognostication a poor prognosis results in possible withdrawal of care and subsequent death for the patient. Hence radiologists would reasonably be cautious to predict poor outcomes resulting in an overall high sensitivity and low specificity in our qualitative models.

However, we expected the qualitative model sensitivity to be much closer to 100% due to the reasons above, but our qualitative model sensitivity was around 90% for all testing groups. The low sensitivity may be attributed to a possible anchoring bias in which radiologists may initially assess patients to be in a poorer neurological state if they have a poor general prognosis. A modeling error may serve as another reasonable explanation for these findings. Our model calculated the optimal threshold for the MRI report grades, which included the cortical only and diffuse anoxic injury grades as predictors of poor neurological outcome. When we qualified the MRI reports, reports received a grade of 1 or 2 if the report contained any mention/indication of diffuse or cortical anoxic injury, respectively. This may have inflated the number of poor outcome predictions in this model by ultimately classifying reports as poor outcome predictors, even if findings of anoxic injury may have been subtle.

Comparison of Quantitative and Qualitative Prediction Models

In general, we found that our qualitative MRI report-based models did not statistically differ from the quantitative ADC value-based models in the prediction of post-cardiac arrest TTM comatose patient neurological recovery. The whole brain region models AUROC as well as all cortical region AUROC did not statistically differ from the

MRI report-based models. The only exception to this is the group 3 occipital lobe-based model. The high predictive value of the occipital lobe models is as explained above. One possible explanation as to why only the group 3 occipital lobe model performed significantly better than its counterpart qualitative model could be the outcome classifier used. In testing group 3, the followed commands value was used instead of the cerebral performance category score as the indicator of outcome. This could have excluded patients who died of non-neurological causes. These findings may again allude to the possibility of a small bias in radiological reports, in which radiologists may assess patients to have poorer neurological health if they have a poorer general prognosis.

Our quantitative ADC value-based models, when sensitivity for a good outcome was forced to 100%, had a much higher specificity for a good outcome than the qualitative models. Positive predictive values for good outcomes were also lower in quantitative models, with negative predictive values being higher than in the qualitative models. This trend was consistent regardless the of testing group or region of interest. Our quantitative model's specificity and negative predictive value for good neurological outcomes may have been greater than the qualitative model's because of its lack of exposure to the biases mentioned above. This general lack of specificity limits the predictive power of both our qualitative and quantitative models. The lack of specificity and positive predictive value for a good outcome of our quantitative model could be explained by the early timing that images were taken. One study similarly modeled outcome prediction using ADC values of MRI images that were 2 to 7 days post-cardiac arrest with high specificity (Hirsch et al., 2020). Taking this into consideration, possibly

assessing quantitative values at a date later than 72 hours may offer more insight into patient outcomes and a higher specificity due to anoxic injury pathways being able to continue days after cardiac arrest (Pulsinelli 1985). Another possible reason why the qualitative model's specificity for a good outcome was much lower and the negative predictive value was lower than the quantitative model's is that the MRI reports were available to the patient care teams. This could mean care teams were likely to contribute to a "self-fulfilling prophecy" in that patients with an MRI report identifying anoxic injury were more likely to have the withdrawal of life sustaining therapy administered to them, even without proper a true diagnosis of anoxic injury.

A combined model may help traditional MRI readings reduce the risk of bias that may be present in qualitative MRI reports and increase the sensitivity to a good neurological outcome, as well as benefit from the combined increase in positive and negative predictive values. However, considering the substantial agreement shown between the most valuable cortical quantitative models and the qualitative models, a different approach may need to be considered when combining the two models to produce a more powerful and accurate prediction tool.

Limitations

Limitations to our study include the confounding factors assessed above, which are present in any similar retrospective study. The fact that a vast majority of our patient population was dead upon 6 months post-cardiac arrest neurological assessment, with a large proportion of those being due to withdrawal of life sustaining therapy,

increases the likelihood of involvement of self-fulfilling prophecy as a confounding factor. Our patient cohort could have been subject to selection bias as well. We were limited to patients who had undergone MRIs. This excludes patients from our cohort that recover consciousness, are critically ill and too unstable to proceed with an MRI, or die before testing can occur.

Another limitation of our study was due to diffusion-weighted imaging having poor noise characteristics in brain regions towards the base of the skull (Alexander et al., 1997). This limitation is also extended to structures within the mesial temporal lobe (Verduin et al., 2021), which restrained hippocampal modeling and analyzation. One MRI study per patient also limited us from analyzing the progression of ADC values, which would have strengthened our models' predictive value by making trends in recovery available to us. Another way we could have strengthened our model's predictive value is to qualify MRI reports with a more robust grading system. Giving grades based on not only anoxic injury location but also severity may help achieve this. Grading done by an expert in the field may help increase qualitative accuracy as well. For example, in one study, two neuroradiologists assessed DWI-imaged brain regions on an anoxic severity scale of 0-4. Scores were added up for the whole brain, cortex structures, and deep gray nuclei structures, any disagreements were discussed to gain a consensus (Keijzer et al., 2020). This method may prove to be more effective for model construction in future studies.

CONCLUSION

Diffusion-weighted imaging plays a crucial role in neuroprognosis in post-cardiac arrest patients. Assessing the presence and extent of anoxic brain injury is paramount in guiding patient care and improving neurological outcomes. Our study provides additional evidence of the importance that quantitative models hold during the prognosis of post-cardiac arrest comatose TTM patients. Based on our model, we saw that bias and self-fulfilling prophecy may influence qualitative reports, however, further research is needed to confirm this. As our models stand, a combined qualitative and quantitative model may not help increase the prognostic value of diffusion-weighted imaging.

Future directions for this study could include changing our modeling tactics so that a combined qualitative and quantitative model of value could be produced. The inclusion of magnetic resonance spectroscopy into our study may also be able to offer not only more predictive value but further insight into recovery, such as regionalized metabolic effects of anoxic brain injury. Expanding our patient cohort to increase our study power may also allow us to detect more quantitative changes.

BIBLIOGRAPHY

Alexander, A. L., Tsuruda, J. S., & Parker, D. L. (1997). Elimination of eddy current artifacts in diffusion-weighted echo-planar images: The use of bipolar gradients. *Magnetic Resonance in Medicine*, 38(6), 1016–1021.

America, I. of M. (US) C. on Q. of H. C. in, Kohn, L. T., Corrigan, J. M., & Donaldson, M. S. (2000). Errors in Health Care: A Leading Cause of Death and Injury. *To Err is Human: Building a Safer Health System*. National Academies Press (US).

Andersen, L. W., Holmberg, M. J., Berg, K. M., Donnino, M. W., & Granfeldt, A. (2019). In-Hospital Cardiac Arrest. *Journal of the American Medical Association*, 321(12), 1200–1210.

Beyers, M. B., Scirica, B. M., Avery, K. R., Henderson, G. V., Lin, A. P., & Lee, J. W. (2018). Combination of clinical exam, MRI and EEG to predict outcome following cardiac arrest and targeted temperature management. *Neurocritical Care*, 29(3), 396–403.

Blackman, J. A., Patrick, P. D., Buck, M. L., & Rust, R. S. (2004). Paroxysmal autonomic instability with dystonia after brain injury. *Archives of Neurology*, 61(3), 321–328.

Choi, J. Y., Choi, Y. S., Rha, D.-W., & Park, E. S. (2016). The clinical outcomes of deep gray matter injury in children with cerebral palsy in relation with brain magnetic resonance imaging. *Research in Developmental Disabilities*, 55, 218–225.

Choi, S. P., Park, K. N., Park, H. K., Kim, J. Y., Youn, C. S., Ahn, K. J., & Yim, H. W. (2010). Diffusion-weighted magnetic resonance imaging for predicting the clinical outcome of comatose survivors after cardiac arrest: A cohort study. *Critical Care*, 14(1), R17.

Collins DL, Neelin P, Peters TM, Evans AC. Automatic 3D intersubject registration of MR volumetric data in standardized Talairach space. *Journal of Computer Assisted Tomography*. 1994;18:192–205

Cronberg, T., Greer, D. M., Lilja, G., Moulaert, V., Swindell, P., & Rossetti, A. O. (2020). Brain injury after cardiac arrest: From prognostication of comatose patients to rehabilitation. *Lancet Neurology*, *19*(7), 611–622.

Dallessio, L. (2020). Post-Cardiac Arrest Syndrome. *Advanced Critical Care*, *31*(4), 383–393.

Desikan RS, Ségonne F, Fischl B, Quinn BT, Dickerson BC, Blacker D, Buckner RL, Dale AM, Maguire RP, Hyman BT, Albert MS, Killiany RJ. An automated labeling system for subdividing the human cerebral cortex on MRI scans into gyral based regions of interest. *Neuroimage*. 2006 Jul 1;31(3):968-80.

Dragancea, I., Wise, M. P., Al-Subaie, N., Cranshaw, J., Friberg, H., Glover, G., Pellis, T., Rylance, R., Walden, A., Nielsen, N., Cronberg, T., & TTM trial investigators. (2017). Protocol-driven neurological prognostication and withdrawal of life-sustaining therapy after cardiac arrest and targeted temperature management. *Resuscitation*, *117*, 50–57.

Ebner, M., Wang, G., Li, W., Aertsen, M., Patel, P. A., Aughwane, R., Melbourne, A., Doel, T., Dymarkowski, S., De Coppi, P., David, A. L., Deprest, J., Ourselin, S., Vercauteren, T. (2020). An automated framework for localization, segmentation and super-resolution reconstruction of fetal brain MRI. *NeuroImage*, *206*, 116324.

Ebner, M., Wang, G., Li, W., Aertsen, M., Patel, P. A., Aughwane, R., Melbourne, A., Doel, T., Dymarkowski, S., De Coppi, P., David, A. L., Deprest, J., Ourselin, S., & Vercauteren, T. (2020). An automated framework for localization, segmentation and super-resolution reconstruction of fetal brain MRI. *NeuroImage*, 206, 116324.

Ebner, M., Chung, K. K., Prados, F., Cardoso, M. J., Chard, D. T., Vercauteren, T., Ourselin, S. (2018). Volumetric reconstruction from printed films: Enabling 30 year longitudinal analysis in MR neuroimaging. *NeuroImage*, 165, 238–250.

Endisch, C., Westhall, E., Kenda, M., Streitberger, K. J., Kirkegaard, H., Stenzel, W., Storm, C., Ploner, C. J., Cronberg, T., Friberg, H., Englund, E., & Leithner, C. (2020). Hypoxic-ischemic encephalopathy evaluated by brain autopsy and neuroprognostication after cardiac arrest. *Journal of American Medical Association Neurology*, 77(11), 1430–1439.

Forgacs, P. B., Devinsky, O., & Schiff, N. D. (2020). Independent functional outcomes after prolonged coma following cardiac arrest: a mechanistic hypothesis. *Annals of Neurology*, 87(4), 618–632.

Frazier JA, Chiu S, Breeze JL, Makris N, Lange N, Kennedy DN, Herbert MR, Bent EK, Koneru VK, Dieterich ME, Hodge SM, Rauch SL, Grant PE, Cohen BM, Seidman LJ, Caviness VS, Biederman J. Structural brain magnetic resonance imaging of limbic and thalamic volumes in pediatric bipolar disorder. *American Journal of Psychiatry*. 2005 Jul;162(7):1256-65

Geocadin, R. G., Koenig, M. A., Jia, X., Stevens, R. D., & Peberdy, M. A. (2008). Management of brain injury after resuscitation from cardiac arrest. *Neurologic Clinics*, 26(2), 487–506, ix.

Gill, R., Teitcher, M., & Ruland, S. (2021). Chapter 19—Neurologic complications of cardiac arrest. In J. Biller (Ed.), *Handbook of Clinical Neurology* (Vol. 177, pp. 193–209). Elsevier.

Goldstein JM, Seidman LJ, Makris N, Ahern T, O'Brien LM, Caviness VS Jr, Kennedy DN, Faraone SV, Tsuang MT. Hypothalamic abnormalities in schizophrenia: sex effects and genetic vulnerability. *Biology Psychiatry*. 2007 Apr 15;61(8):935-45

Grace, P. A. (1994). Ischaemia-reperfusion injury. *The British Journal of Surgery*, 81(5), 637–647.

Granfeldt, A., Holmberg, M. J., Nolan, J. P., Soar, J., & Andersen, L. W. (2021). Targeted temperature management in adult cardiac arrest: Systematic review and meta-analysis. *Resuscitation*, 167, 160–172.

Gräsner, J.-T., Lefering, R., Koster, R. W., Masterson, S., Böttiger, B. W., Herlitz, J., Wnent, J., Tjelmeland, I. B. M., Ortiz, F. R., Maurer, H., Baubin, M., Mols, P., Hadžibegović, I., Ioannides, M., Škulec, R., Wissenberg, M., Salo, A., Hubert, H., Nikolaou, N. I., ... EuReCa ONE Collaborators. (2016). EuReCa ONE-27 Nations, ONE Europe, ONE Registry: A prospective one month analysis of out-of-hospital cardiac arrest outcomes in 27 countries in Europe. *Resuscitation*, 105, 188–195.

Helenius, J., Soinne, L., Perkiö, J., Salonen, O., Kangasmäki, A., Kaste, M., Carano, R. A. D., Aronen, H. J., & Tatlisumak, T. (2002). Diffusion-weighted MR imaging in normal human brains in various age groups. *American Journal of Neuroradiology*, 23(2), 194–199.

Hirsch, K. G., Fischbein, N., Mlynash, M., Kemp, S., Bammer, R., Eyngorn, I., Tong, J., Moseley, M., Venkatasubramanian, C., Caulfield, A. F., & Albers, G. (2020). Prognostic

value of diffusion-weighted MRI for post-cardiac arrest coma. *Neurology*, 94(16), e1684–e1692.

Hirsch, K. G., Mlynash, M., Jansen, S., Persoon, S., Eynhorn, I., Krasnokutsky, M. V., Wijman, C. A. C., & Fischbein, N. J. (2015). Prognostic value of a qualitative brain MRI scoring system after cardiac arrest. *Journal of Neuroimaging*, 25, 430–437.

Hoiland, R. L., Rikhranj, K. J. K., Thiara, S., Fordyce, C., Kramer, A. H., Skrifvars, M. B., Wellington, C. L., Griesdale, D. E., Fergusson, N. A., & Sekhon, M. S. (2022). Neurologic Prognostication After Cardiac Arrest Using Brain Biomarkers: A Systematic Review and Meta-analysis. *Journal of American Medical Association Neurology*, 79(4), 390–398.

Howell, K., Grill, E., Klein, A.-M., Straube, A., & Bender, A. (2013). Rehabilitation outcome of anoxic-ischaemic encephalopathy survivors with prolonged disorders of consciousness. *Resuscitation*, 84(10), 1409–1415.

Hua et al., Tract probability maps in stereotaxic spaces: analysis of white matter anatomy and tract-specific quantification. *NeuroImage*, 39(1):336-347 (2008)

Huang, B. Y., & Castillo, M. (2008). Hypoxic-ischemic brain injury: Imaging findings from birth to adulthood. *Radiographics: A Review Publication of the Radiological Society of North America, Inc*, 28(2), 417–439; quiz 617.

Imberti, R., Bellinzona, G., Riccardi, F., Pagani, M., & Langer, M. (2003). Cerebral perfusion pressure and cerebral tissue oxygen tension in a patient during cardiopulmonary resuscitation. *Intensive Care Medicine*, 29(6), 1016–1019.

Ishii, K., Sasaki, M., Kitagaki, H., Sakamoto, S., Yamaji, S., & Maeda, K. (1996). Regional difference in cerebral blood flow and oxidative metabolism in human cortex. *Journal of Nuclear Medicine: Official Publication, Society of Nuclear Medicine*, 37(7), 1086–1088.

Kamps, M. J. A., Horn, J., Oddo, M., Fugate, J. E., Storm, C., Cronberg, T., Wijman, C. A., Wu, O., Binnekade, J. M., & Hoedemaekers, C. W. E. (2013). Prognostication of neurologic outcome in cardiac arrest patients after mild therapeutic hypothermia: A meta-analysis of the current literature. *Intensive Care Medicine*, 39(10), 1671–1682.

Kang, Y. (2019). Management of post-cardiac arrest syndrome. *Acute and Critical Care*, 34(3), 173–178.

Keijzer, H. M., Verhulst, M., Meijer, F. J. A., Tonino, B. A. R., Bosch, F. H., Klijn, C. J. M., Hoedemaekers, C. W. E., & Hofmeijer, J. (2022). Prognosis After Cardiac Arrest: The Additional Value of DWI and FLAIR to EEG. *Neurocritical Care*, 37(1), 302–313.

Lacerte, M., Hays Shapshak, A., & Mesfin, F. B. (2022). Hypoxic Brain Injury. In *StatPearls*.

Laver, S., Farrow, C., Turner, D., & Nolan, J. (2004). Mode of death after admission to an intensive care unit following cardiac arrest. *Intensive Care Medicine*, 30(11), 2126–2128.

Lee, C. S., Nagy, P. G., Weaver, S. J., & Newman-Toker, D. E. (2013). Cognitive and system factors contributing to diagnostic errors in radiology. *AJR. American Journal of Roentgenology*, 201(3), 611–617.

Louis, E. K. S., Frey, L. C., Britton, J. W., Frey, L. C., Hopp, J. L., Korb, P., Koubeissi, M. Z., Lievens, W. E., Pestana-Knight, E. M., & Louis, E. K. S. (2016). Introduction. In *Electroencephalography (EEG): An Introductory Text and Atlas of Normal and Abnormal Findings in Adults, Children, and Infants*. American Epilepsy Society.

Macrae, C. N., & Quadflieg, S. (2012). *Encyclopedia of Human Behavior* – 2nd edition.

Madl, C., & Holzer, M. (2004). Brain function after resuscitation from cardiac arrest. *Current Opinion in Critical Care*, 10(3), 213–217.

Madl, C., Kramer, L., Yeganehfar, W., Eisenhuber, E., Kranz, A., Ratheiser, K., Zauner, C., Schneider, B., & Grimm, G. (1996). Detection of nontraumatic comatose patients with no benefit of intensive care treatment by recording of sensory evoked potentials. *Archives of Neurology*, 53(6), 512–516.

Makris N, Goldstein JM, Kennedy D, Hodge SM, Caviness VS, Faraone SV, Tsuang MT, Seidman LJ. Decreased volume of left and total anterior insular lobule in schizophrenia. *Schizophrenia Research*. 2006 Apr;83(2-3):155-71

McHugh, M. L. (2012). Interrater reliability: The kappa statistic. *Biochemia Medica*, 22(3), 276–282.

Mehra, R. (2007). Global public health problem of sudden cardiac death. *Journal of Electrocardiology*, 40(6, Supplement 1), S118–S122.

Mlynash, M., Campbell, D. M., Leproust, E. M., Fischbein, N. J., Bammer, R., Eyngorn, I., Hsia, A. W., Moseley, M., & Wijman, C. A. C. (2010). Temporal and spatial profile of brain diffusion-weighted MRI after cardiac arrest. *Stroke; a Journal of Cerebral Circulation*, 41(8), 1665–1672.

Mongardon, N., Perbet, S., Lemiale, V., Dumas, F., Poupet, H., Charpentier, J., Péne, F., Chiche, J.-D., Mira, J.-P., & Cariou, A. (2011). Infectious complications in out-of-hospital cardiac arrest patients in the therapeutic hypothermia era. *Critical Care Medicine*, 39(6), 1359–1364.

Mori et al., MRI atlas of human white matter. *Elsevier*, Amsterdam, The Netherlands (2005)

Nguyen, P. L., Alreshaid, L., Poblete, R. A., Konye, G., Marehbian, J., & Sung, G. (2018). Targeted temperature management and multimodality monitoring of comatose patients after cardiac arrest. *Frontiers in Neurology*, 9, 768.
<https://doi.org/10.3389/fneur.2018.00768>

Nobile, L., Taccone, F. S., Szakmany, T., Sakr, Y., Jakob, S. M., Pellis, T., Antonelli, M., Leone, M., Wittebole, X., Pickkers, P., & Vincent, J.-L. (2016). The impact of extracerebral organ failure on outcome of patients after cardiac arrest: An observational study from the ICON database. *Critical Care*, 20, 368.

Nolan, J. P., Neumar, R. W., Adrie, C., Aibiki, M., Berg, R. A., Böttiger, B. W., Callaway, C., Clark, R. S. B., Geocadin, R. G., Jauch, E. C., Kern, K. B., Laurent, I., Longstreth, W. T., Merchant, R. M., Morley, P., Morrison, L. J., Nadkarni, V., Peberdy, M. A., Rivers, E. P., ... Hoek, T. V. (2008). Post-cardiac arrest syndrome: Epidemiology, pathophysiology, treatment, and prognostication. A Scientific Statement from the International Liaison Committee on Resuscitation; the American Heart Association Emergency Cardiovascular Care Committee; the Council on Cardiovascular Surgery and Anesthesia; the Council on Cardiopulmonary, Perioperative, and Critical Care; the Council on Clinical Cardiology; the Council on Stroke. *Resuscitation*, 79(3), 350–379.

Oku, K., Kuboyama, K., Safar, P., Obrist, W., Sterz, F., Leonov, Y., & Tisherman, S. A. (1994). Cerebral and systemic arteriovenous oxygen monitoring after cardiac arrest. Inadequate cerebral oxygen delivery. *Resuscitation*, 27(2), 141–152.

Panchal, A. R., Bartos, J. A., Cabañas, J. G., Donnino, M. W., Drennan, I. R., Hirsch, K. G., Kudenchuk, P. J., Kurz, M. C., Lavonas, E. J., Morley, P. T., O’Neil, B. J., Peberdy, M. A., Rittenberger, J. C., Rodriguez, A. J., Sawyer, K. N., Berg, K. M., & Adult Basic and Advanced Life Support Writing Group. (2020). Part 3: Adult basic and advanced life support: 2020 American Heart Association guidelines for cardiopulmonary resuscitation and emergency cardiovascular care. *Circulation*, 142(16_suppl_2), S366–S468.

Peberdy, M. A., Kaye, W., Ornato, J. P., Larkin, G. L., Nadkarni, V., Mancini, M. E., Berg, R. A., Nichol, G., & Lane-Trullt, T. (2003). Cardiopulmonary resuscitation of adults in the hospital: A report of 14720 cardiac arrests from the National Registry of Cardiopulmonary Resuscitation. *Resuscitation*, 58(3), 297–308.

Pulsinelli, W. A. (1985). Selective Neuronal Vulnerability: Morphological and Molecular Characteristics**Presented at the Sendai Forum ’84 on Cerebrovascular Accidents. In K. Kogure, K.-A. Hossmann, B. K. Siesjö, & F. A. Welsh (Eds.), *Progress in Brain Research* (Vol. 63, pp. 29–37).

Ramiro, J. I., & Kumar, A. (2015). Updates on Management of anoxic brain injury after cardiac arrest. *Missouri Medicine*, 112(2), 136–141.

Rasmussen, T. P., Bullis, T. C., & Girotra, S. (2020). Targeted Temperature Management for Treatment of Cardiac Arrest. *Current Treatment Options in Cardiovascular Medicine*, 22(11), 39.

Reynolds, E. C., & Soar, J. (2014). How are cerebral performance category scores measured for audit and research purposes? *Resuscitation*, *85*(5), e73–e74.

Rossetti, A. O., Rabinstein, A. A., & Oddo, M. (2016). Neurological prognostication of outcome in patients in coma after cardiac arrest. *The Lancet. Neurology*, *15*(6), 597–609.

Sandroni, C., Cronberg, T., & Sekhon, M. (2021). Brain injury after cardiac arrest: Pathophysiology, treatment, and prognosis. *Intensive Care Medicine*, *47*(12), 1393–1414.

Sandroni, C., D'Arrigo, S., & Nolan, J. P. (2018). Prognostication after cardiac arrest. *Critical Care*, *22*(1), 150.

Schaaf, K. P. W., Artman, L. K., Peberdy, M. A., Walker, W. C., Ornato, J. P., Gossip, M. R., & Kreutzer, J. S. (2013). Anxiety, depression, and PTSD following cardiac arrest: A systematic review of the literature. *Resuscitation*, *84*(7), 873–877.

Sener, R. N. (2001). Diffusion MRI: Apparent diffusion coefficient (ADC) values in the normal brain and a classification of brain disorders based on ADC values. *Computerized Medical Imaging and Graphics*, *25*(4), 299–326.

Shokri-Kojori, E., Tomasi, D., Alipanahi, B., Wiers, C. E., Wang, G.-J., & Volkow, N. D. (2019). Correspondence between cerebral glucose metabolism and BOLD reveals relative power and cost in human brain. *Nature Communications*, *10*(1), Article 1.

Snider, S. B., Fischer, D., McKeown, M. E., Cohen, A. L., Schaper, F. L. W. V. J., Amorim, E., Fox, M. D., Scirica, B., Bevers, M. B., & Lee, J. W. (2022). Regional distribution of brain injury after cardiac arrest: clinical and electrographic correlates. *Neurology*, *98*(12), e1238–e1247.

Stammet, P., Collignon, O., Hassager, C., Wise, M. P., Hovdenes, J., Åneman, A., Horn, J., Devaux, Y., Erlinge, D., Kjaergaard, J., Gasche, Y., Wanscher, M., Cronberg, T., Friberg, H., Wetterslev, J., Pellis, T., Kuiper, M., Gilson, G., Nielsen, N., & TTM-Trial Investigators. (2015). Neuron-specific enolase as a predictor of death or poor neurological outcome after out-of-hospital cardiac arrest and targeted temperature management at 33°C and 36°C. *Journal of the American College of Cardiology*, 65(19), 2104–2114.

Stern, P., Bartos, V., Uhrova, J., Bezdickova, D., Vanickova, Z., Tichy, V., Pelinkova, K., Prusa, R., & Zima, T. (2007). Performance characteristics of seven neuron-specific enolase assays. *Tumour Biology: The Journal of the International Society for Oncodevelopmental Biology and Medicine*, 28(2), 84–92.

Taccone, F. S., Picetti, E., & Vincent, J.-L. (2020). High quality targeted temperature management (TTM) after cardiac arrest. *Critical Care*, 24(1), 6.

This repository takes clinical T1 (T2, FLAIR) and DWI BIDS-formatted data and prepares it for lesion tracing. (2022). [Shell]. Boston Children’s Hospital Laboratory of Translational Neuroimaging. https://github.com/bchcohenlab/bids_lesion_code (Original work published 2020)

van Veen, E., van der Jagt, M., Citerio, G., Stocchetti, N., Gommers, D., Burdorf, A., Menon, D. K., Maas, A. I. R., Kompanje, E. J. O., & Lingsma, H. F. (2021). Occurrence and timing of withdrawal of life-sustaining measures in traumatic brain injury patients: A CENTER-TBI study. *Intensive Care Medicine*, 47(10), 1115–1129.

Verduin, M., Primakov, S., Compter, I., Woodruff, H. C., van Kuijk, S. M. J., Ramaekers, B. L. T., te Dorsthorst, M., Revenich, E. G. M., ter Laan, M., Pegge, S. A. H., Meijer, F. J. A., Beckervordersandforth, J., Speel, E. J., Kusters, B., de Leng, W. W.

J., Anten, M. M., Broen, M. P. G., Ackermans, L., Schijns, O. E. M. G., ... Hoeben, A. (2021). Prognostic and Predictive Value of Integrated Qualitative and Quantitative Magnetic Resonance Imaging Analysis in Glioblastoma. *Cancers*, 13(4), 722.

Visualizing the Performance of Scoring Classifiers. (n.d.). Retrieved February 21, 2023, from <https://ipa-tys.github.io/ROCR/>

Waite, S., Scott, J., Gale, B., Fuchs, T., Kolla, S., & Reede, D. (2017). Interpretive Error in Radiology. *AJR. American Journal of Roentgenology*, 208(4), 739–749.

Wakana et al., Reproducibility of quantitative tractography methods applied to cerebral white matter. *NeuroImage* 36:630-644 (2007)

Westhall, E., Rossetti, A. O., van Rootselaar, A. F., Wesenberg Kjaer, T., Horn, J., Ullen, S., Friberg, H., Nielsen, N., Rosen, I., Aneman, A., Erlinge, D., Gasche, Y., Hassager, C., Hovdenes, J., Kjaergaard, J., Kuiper, M., Pellis, T., Stammet, P., Wanscher, M., ... Investigators, T. T. (2016). Standardized EEG interpretation accurately predicts prognosis after cardiac arrest. *Neurology*, 86, 1482–1490.

Yenari, M. A., & Han, H. S. (2012). Neuroprotective mechanisms of hypothermia in brain ischaemia. *Nature Reviews. Neuroscience*, 13(4), 267–278.

CURRICULUM VITAE

